

New mechanism of singlet-oxygen production in processes with participation of electronically and vibrationally excited ozone molecules

K. S. Klopovskii, A. S. Kovalev, D. V. Lopaev, N. A. Popov, A. T. Rakhimov, and T. V. Rakhimova

D. V. Skobel'tsyn Scientific-Research Institute of Nuclear Physics at M. V. Lomonosov Moscow State University, Moscow, Russia

(Submitted 2 September 1994)

Zh. Éksp. Teor. Fiz. **107**, 1080–1099 (April 1995)

A theoretical model of the production of oxygen molecules in the lower singlet state $a^1\Delta_g$ in excited nitrogen–oxygen gaseous media is presented. The model includes a new mechanism of $O_2(a^1\Delta_g)$ production by means of energy transfer accompanying the interaction of the electronically excited 1^3B_2 state of ozone with ground-state oxygen molecules. It is shown that ozone molecules in the 1^3B_2 state are produced mainly by nonadiabatic transitions from the $1A_1$ ground state as a result of strong excitation of asymmetric vibrations of O_3 . It is shown that vibrationally excited nitrogen plays an important role as a reservoir for asymmetric vibrations of ozone. The observed acceleration of the quenching of $O_2(a^1\Delta_g)$ molecules in reactions with ozone is associated with the excitation of bending vibrations of O_3 and probably proceeds via the excitation of the intermediate electronic state $O_3(1^3B_2)$. The rate constants for previously unknown processes were determined by comparing the modeling results to experimental data. Values were obtained for the rate constants of vv' exchange between $N_2(\nu=1)$ and $O_3(101)$ and for quasiresonant transfer of electronic excitation from $O_3(1^3B_2)$ to $O_2(a^1\Delta_g)$: $(5 \pm 2) \cdot 10^{-14}$ cm³/s and $(1.4 \pm 0.5) \cdot 10^{-12}$ cm³/s, respectively. © 1995 American Institute of Physics.

1. INTRODUCTION

Singlet oxygen molecules are oxygen molecules excited to the lowest metastable level $a^1\Delta_g$ (the excitation energy is 0.977 eV). This level is long-lived and its radiative lifetime is ≈ 4700 s.¹ The long radiative lifetime and the low quenching rate of singlet oxygen $O_2(a^1\Delta_g)$ allow for efficient accumulation of these molecules in a gaseous medium, and this makes possible long-time storage of energy in electronic levels of molecular oxygen.

This feature of singlet oxygen is used to achieve inversion in the $5^2P_{1/2} \rightarrow 5^2P_{3/2}$ transition of atomic iodine in an oxygen-iodine laser.²

The development of electric-discharge methods for pumping an oxygen-iodine laser stimulated a search for conditions that would make it possible to obtain the high concentration of metastable oxygen molecules $O_2(a^1\Delta_g)$ (more than 17–20%) that is required for inversion of a transition in atomic iodine.^{3–7}

These investigations reveal that for high $O_2(a^1\Delta_g)$ concentrations, the conductivity of the gas-discharge plasma can increase because electron detachment from negative ions is accelerated,^{8,9} which can therefore change the conditions under which discharges burn. This effect is fundamental for the development of an entire class of gas-discharge devices employing oxygen as a component of the working medium—ozonizers, plasma-chemical reactors in microelectronics, etc. It should be noted that gas-discharge methods for excitation of a medium open up new ways to investigate processes involving singlet oxygen under strongly nonequilibrium conditions.

Singlet oxygen is one of the most important components

in the earth's upper atmosphere. The luminescence of $O_2(a^1\Delta_g)$ molecules determines the intensity of IR emissions of the atmosphere near 1.27 μm , which are strongest in the daytime and nighttime sky glow.¹ Note that the question of the mechanism of singlet oxygen production in the amounts required to explain the observed intensity of IR emissions of the atmosphere is still open.

The kinetics of singlet oxygen in the earth's atmosphere is closely associated with the kinetics of atmospheric ozone. The main source of singlet oxygen in the earth's atmosphere is ozone photolysis in the Hartley band (200–310 nm); this is the main channel for the production of $O_2(a^1\Delta_g)$ and atomic oxygen in the excited state $1D$. The interaction of $O_2(a^1\Delta_g)$ molecules with ozone molecules in turn results in the destruction of ozone molecules.

The great progress achieved over the last few years in laboratory investigations has appreciably expanded our understanding of the kinetics of processes in a strongly nonequilibrium oxygen-containing medium. There is an extensive literature on investigations of processes resulting in the production and destruction of singlet-oxygen molecules as well as energy transformation processes in a nonequilibrium oxygen-containing medium.^{2–12}

In a gas-discharge plasma the $O_2(a^1\Delta_g)$ molecules are excited in inelastic interactions of electrons with oxygen molecules. In experiments in a drift chamber,^{3–5} however, the rate of $O_2(a^1\Delta_g)$ production was found to be higher than by direct electron impact. To explain this, cascade processes which populate the electronic level $a^1\Delta_g$ from higher-lying electronic states $c^1\Sigma_u^-$ and $b^1\Sigma_g^+$ were introduced into the analysis.^{3–5}

A number of pulsed-discharge experiments yielded re-

sults that could not be explained by cascade filling of the $a^1\Delta_g$ state.^{6,10-12} For example, in Ref. 6 the $O_2(a^1\Delta_g)$ kinetics with the excitation of a nitrogen–oxygen mixture by a self-sustained volume discharge was investigated. Comparing the results of numerical modeling to the experimental data showed⁶ that to explain the observed high $O_2(a^1\Delta_g)$ concentration some mechanism for transforming the vibrational energy stored in nitrogen into excitation energy of the $a^1\Delta_g$ electronic level of the oxygen molecule must be introduced. The investigation of the kinetics of singlet-oxygen production in the afterglow of an externally driven discharge in a $N_2:O_2$ mixture¹⁰ (in which $\approx 95\%$ of the energy fed into the discharge is stored in the vibrational degrees of freedom of the nitrogen molecules) confirm the hypothesis of Ref. 6.

The need to clarify the mechanism of such efficient $O_2(a^1\Delta_g)$ production in excited nitrogen–oxygen mixtures as well as the lack of an adequate kinetic model of this phenomenon stimulated a series of experimental investigations.^{11,12}

In the experiments of Refs. 11 and 12 the time dependence of the $O_2(a^1\Delta_g)$ concentration was investigated both with mixing of nitrogen and oxygen flows excited separately by hf discharges and with the excitation of a $N_2:O_2$ mixture. It was found that the emission of $O_2(a^1\Delta_g)$ molecules after the excited nitrogen and oxygen flows are mixed is nonmonotonic. This nonmonotonicity can be interpreted as the appearance of an additional $O_2(a^1\Delta_g)$ production channel. Analysis of the experimental data of Refs. 11 and 12 made it possible to determine the general role of vibrationally excited ozone in the mechanism of $O_2(a^1\Delta_g)$ production.

Anomalous behavior of $O_2(a^1\Delta_g)$ luminescence was also observed under different experimental conditions in Ref. 13, where $O_2(a^1\Delta_g)$ production with an admixture of molecular oxygen in a nitrogen flow containing $O_2(a^1\Delta_g)$ atoms was studied. A high rate of $O_2(a^1\Delta_g)$ production, corresponding to the production rates of singlet oxygen in the earth's atmosphere, was observed. Note that the data of Ref. 13, like the results of Refs. 11 and 12, cannot be explained on the basis of currently existing kinetic models.

In the present paper we propose a new kinetic model that makes it possible to explain existing experimental data on $O_2(a^1\Delta_g)$ production and destruction in excited nitrogen–oxygen mixtures on the basis of a single system of processes which includes reactions in which electronically and vibrationally excited ozone molecules participate.

2. MODELING OF CHEMICAL PROCESSES OCCURRING DURING THE MIXING OF EXCITED NITROGEN AND OXYGEN FLOWS

The new kinetic model of singlet-oxygen production by mixing of independently excited gas which is described in the present paper stems from a comparison of numerical calculations with a large array of experimental data.^{11,12}

The experiments of Refs. 11 and 12 studied the dynamics of the $O_2(a^1\Delta_g)$ concentration in connection with both mixing of nitrogen and oxygen flows excited separately by hf discharges and excitation of a $N_2:O_2$ mixture. It was shown that the rate of $O_2(a^1\Delta_g)$ production during mixing of excited nitrogen and oxygen flows is proportional to the O_2

concentration. Moreover, it was observed that the $O_2(a^1\Delta_g)$ emission is nonmonotonic; this can be interpreted as the appearance of additional $O_2(a^1\Delta_g)$ production channels. It was shown that the degree of nonmonotonicity decreases with increasing oxygen fraction in the mixture as well as with the deactivation of the vibrational excitation of nitrogen molecules. The nonmonotonicity of the emission vanished if $O(^3P)$ oxygen atoms and, correspondingly, ozone molecules are artificially “removed” from the mixing zone.

In the first stage of the numerical modeling of the experiments of Refs. 11 and 12, the degree of nonequilibrium excitation and dissociation of each of the gases in the hf discharges was calculated, followed by relaxation of this excitation during transport of the gases to the mixing zone. These data were used as the initial conditions for calculating the dynamics of the mixture composition after the excited nitrogen and oxygen flows are mixed.

In the modeling of hf discharges a self-consistent calculation was performed of the electron energy distribution function and the system of kinetic equations was solved for the charged and neutral components of the plasma in the local-effective-field approximation. In the calculations the sets of cross sections for the interaction of electrons with oxygen and nitrogen molecules were used, like the set employed in Ref. 9, including the cross sections obtained in Ref. 6 for the dissociation of O_2 molecules by electron impact.

The effective reduced fields E/N in hf discharges in N_2 and O_2 were determined so as to obtain the best agreement between the computed and experimentally measured values of the current densities, the specific energy input, the gas temperature, and the $O_2(a^1\Delta_g)$ and $O_2(b^1\Sigma_g^+)$ concentrations. Note that the values found for E/N are in good agreement with the value of the effective field in the positive column of the discharge determined by a self-consistent model of an hf discharge in oxygen,⁹ which included a calculation of the electric field in the interelectrode gap, taking into account the nonlocal nature of the electron energy distribution function, as well as the spatial distributions of the charged and neutral particles. The occupancies of the lower vibrational levels of the N_2 molecules were found by solving the system of equations describing the vibrational kinetics of individual levels.

The collections of cross sections for the interaction of electrons with nitrogen and oxygen molecules as well as data on the rates of the known chemical reactions, which are employed in the present paper, have been tested many times by comparing the calculations and experimental data.^{6,7,9,11}

The occupancies of the electronic and vibrational states of nitrogen and oxygen molecules, which were determined by modeling the action of hf discharges on each of these gases and their subsequent transport up to the mixing zone, were used as input data for the equations of chemical kinetics, which describe the processes occurring in the mixing zone of the gas flows.

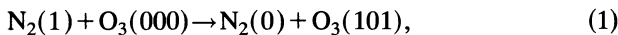
2.1. Kinetic scheme

The kinetic scheme included reactions involving particles whose characteristic lifetimes (collisional and radiative) were longer than the corresponding transport times of the gases up to the mixing zone. To model the $O_2(a^1\Delta_g)$ kinetics in the mixing zone under the experimental conditions of Refs. 11 and 12, it is sufficient to take into account processes involving the following particles: $O_2(a^1\Delta_g)$, $O_2(b^1\Sigma_g^+)$, $O(^3P)$, $O_3(v_1, v_2, v_3)$, and $N_2(X^1\Sigma_g^+, v)$. Here, $N_2(X^1\Sigma_g^+, v)$ are nitrogen molecules in the v th vibrational level of the electronic ground state; $O_3(v_1, v_2, v_3)$ are ozone molecules in the ground electronic state $^1A_1(C_{2v})$; v_1, v_2 , and v_3 are the vibrational quanta in the symmetric stretching mode, the symmetric bending mode, and the asymmetric stretching mode, respectively.

It should be noted that the atomic oxygen in the oxygen gas excited in the discharge is almost completely converted into ozone as it flows into the mixing zone ($t_{tr} > 40$ ms), since under the conditions studied the characteristic conversion time is 15 ms. The relaxation times for the vibrational excitation of the oxygen molecules under the conditions of Ref. 11 are appreciably shorter than the transport time t_{tr} , and hence there is enough time for the vibrational excitation in the oxygen flow to relax before the mixing zone is reached.

The lack of information about vibrational and relaxation processes in different modes of this system makes it difficult to analyze in detail the kinetics of individual levels in the system consisting of $N_2(v)$ and $O_3(v_1, v_2, v_3)$. The quanta of the ozone stretching vibrations are close in magnitude,^{16,17} so that the vv' exchange rate between the O_3 stretching modes is quite high. This makes it possible to combine the symmetric and asymmetric stretching vibrations of the ozone molecule into a single doubly degenerate mode.^{18,19} In what follows, all quantities referring to the combined mode of O_3 will be marked with the index "a" (asymmetric mode), and the quantities referring to the symmetric bending mode will be marked with the index "s."

We note that under the experimental conditions of Ref. 11, the intramode exchange rates in both O_3 and N_2 are higher than the intermolecular and intramode exchange rates. The vv' vibrational exchange process between N_2 and O_3 in the lower levels has a quasisymmetry character (one vibrational quantum of a nitrogen molecule equals approximately two quanta of stretching vibrations of ozone):



(the rate constant K_1 of this reaction was a parameter of the model). For this reason vv' exchange between the lower vibrational levels of N_2 and O_3 will make the main contribution to the vibrational exchange process. This makes it possible to employ the harmonic-oscillator approximation, and the quasistationary distributions over the vibrational levels in nitrogen and the two modes of ozone can be determined by the vibrational temperatures T_n , T_a , and T_s , respectively.

The approach of Ref. 20 was used to describe the effect of the vibrational excitation of ozone molecules on the rates

of endothermal processes. In this approach the dependence of the microscopic reaction rate constant K_R on the energy E_v of the v th vibrational level has the form

$$k_R(E_v) = k_0 \exp\left\{\left(-\frac{E_{act} - \alpha E_v}{kT}\right)\theta(E_{act} - \alpha E_v)\right\}, \quad (2)$$

where T is the gas temperature, E_{act} is the activation energy of the reaction, $\theta(x)$ is the Heaviside function, k is Boltzmann's constant, k_a is the rate constant for gas-kinetic collisions, and α is an empirical parameter that describes the acceleration of the reaction stimulated by the vibrational excitation as a result of a decrease in the activation barrier by an amount αE_v .

Averaging the relation (2) over a Boltzmann distribution in the vibrational modes of ozone gives the following expression for the reaction rate constant:

$$K = k_0 \exp\left\{-\frac{E_{act}}{\alpha k T_v}\right\} \left[1 + \{\exp(E_{act}\beta) - 1\} \times \frac{1 - \exp(-\hbar\omega/kT_v)}{1 - \exp(-\alpha\hbar\omega\beta)}\right], \quad (3)$$

$$\beta = \left(\frac{1}{\alpha T} - \frac{1}{T}\right)/k,$$

where $\alpha = \alpha_a$ for the asymmetric mode and $\alpha = \alpha_s$ for the symmetric mode and T_v are the vibrational temperatures of the asymmetric T_a or symmetric T_s modes of ozone.

The balance equations for the average number of vibrational quanta "n," "a," and "s" in nitrogen and the doubly degenerate asymmetric and symmetric modes of ozone, respectively, were used to model the vibrational kinetics in the nitrogen-ozone system:

$$\frac{dn}{dt} = -Q_{vv}^{na} - P_{vT}^n, \quad (4)$$

$$\frac{da}{dt} = Q_{vv}^{na} - Q_{vv}^{as} - P_{vT}^a + F^a - D^a, \quad (5)$$

$$\frac{ds}{dt} = Q_{vv}^{as} - P_{vT}^s - G^s + F^s - D^s, \quad (6)$$

where

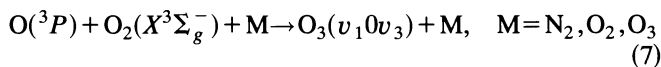
$$n = \frac{[N_2]}{\exp\{\hbar\omega_n/kT_n\} - 1}, \quad a = \frac{2[O_2]}{\exp\{\hbar\omega_a/kT_a\} - 1},$$

$$s = \frac{[O_3]}{\exp\{\hbar\omega_s/kT_s\} - 1},$$

$\hbar\omega_{n,a,s}$ are the corresponding vibrational quanta; Q_{vv}^{na} is the vibrational exchange rate between N_2 and O_3 [reaction No. (1)]; Q_{vv}^{as} is the intermode vv' exchange rate in ozone; P_{vT}^n , P_{vT}^a , and P_{vT}^s are the rates of the vT relaxation reactions of nitrogen and the asymmetric and symmetric modes of ozone; and G^s is determined by the $O_3(v_s)$ decomposition reactions. The processes resulting in the production and destruction of vibrationally excited ozone molecules are designated as $F^{a(s)}$ and $D^{a(s)}$, respectively.

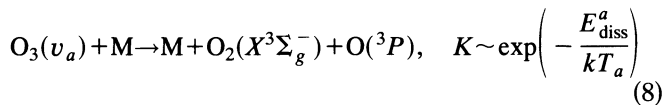
2.2. Processes in which vibrationally excited ozone molecules participate

According to the experimental data of Refs. 21–23, in the three-body reactions

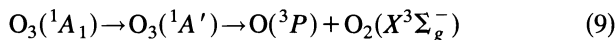


vibrationally excited ozone molecules are produced only in the asymmetric mode. In this connection, the rate F^a of production of O_3 in the asymmetric mode is determined by the reactions (7), and the excitation rate F^s of molecules in the symmetric mode is assumed to be low ($F^s \ll F^a$).

The process of dissociation of vibrationally excited ozone molecules



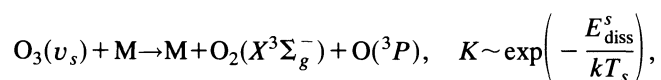
is exactly the inverse of the reaction (7). For this reason, it can be conjectured that the dissociation of vibrationally excited ozone molecules in collisions likewise proceeds predominantly via the asymmetric vibrational mode [D^a is the dissociation rate through the excitation of the asymmetric mode in Eq. (5)]. This assumption is based on the results of quantum-mechanical calculations of the energy surfaces of the O_3 molecule. The results of *ab initio* calculations of the potential surface of the ground state of the ozone molecule for large internuclear distances, which correspond to the dissociation process



are presented in Ref. 22.

It was shown that the energetically most favorable coordinate of the reaction (9) passes through the transitional state $^1A'(C_s)$, in which the angle between the valence bonds is practically equal to the angle in the equilibrium configuration $^1A_1(C_{2v})$ of the O_3 molecule. In the reaction (9) ozone dissociates by means of the rupture of the valence bond with overcoming of the energy barrier $E_a \approx 1.13$ eV.

The results of Ref. 23 indicate that dissociation via the excitation of the symmetric bending vibrational mode (D^s is the dissociation rate in this vibrational mode)



is impeded, since the motion toward the dissociation valley $\text{O}(^3P) + \text{O}_2(X^3\Sigma_g^-)$ along this normal coordinate is associated with overcoming a higher energy barrier $E_s \approx 2$ eV (Ref. 23) than in the case of motion along one of the valence modes, i.e., $D^a \gg D^s$. This is also indicated by the fact that for $\text{O}_3(^1A_1)$ molecules, excited into the asymmetric mode, broadening of the vibrational levels as a result of predissociation is not observed right up to the dissociation limit.¹⁹

In our model the dissociation energy E_{diss}^s of ozone via the bending mode was a parameter, and we assumed $E_{\text{diss}}^s > E_{\text{diss}}^a$.

To describe the dissociation process, it is necessary to know the vibrational distribution function for the upper lev-

els under conditions such that chemical reactions proceed rapidly. As shown in Ref. 20, the vibrational distribution function in the upper levels can be represented in the form

$$f_v \approx f_v^0 \exp\left(-\int_{v^*}^v \frac{K_d(v')[M]dv'}{Q_{vv}(v')[\text{O}_3](1+\xi(v'))}\right), \quad (10)$$

$$K_D = \int_{v^*}^{v_d} f_v' K_d(v') dv'. \quad (11)$$

In Eqs. (10) and (11) the integration extends over the number of the vibrational level; $K_d(v)$ is the microscopic rate constant for collisional dissociation of ozone; $[\text{O}_3]$ and $[\text{M}]$ are, respectively, the ozone concentration and the total particle concentration; $\xi(v) = P_{vT}(v)/Q_{vv}(v)$, where $P_{vT}(v)$ and $Q_{vv}(v)$ are the rate constants for vT and vv processes, respectively, in the upper levels of each vibrational mode of O_3 ; v^* is the vibrational level at which the ozone dissociation process makes an appreciable contribution to the $\text{O}_3(v^*)$ population; and K_D is the total rate constant for collisional dissociation.

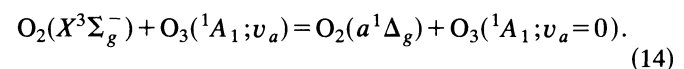
The dependence of the microscopic dissociation rate constant $K_d(v)$ on the vibrational level v was assumed to be of the form (2) with $\alpha = 1$. Carrying out the integration in Eq. (11) gives the following dependence of the dissociation rate constant for ozone on the vibrational temperature T_v :

$$K_D \approx K_0 \exp\left(-\frac{E_{\text{diss}}^v}{T_v}\right) \phi(T_v), \quad (12)$$

$$\phi(T_v) = \exp\left(-\frac{K_0[\text{M}] \exp\left(-\frac{E_{\text{diss}}^v}{T_v}\right)}{Q_{vv}[\text{O}_3]}\right). \quad (13)$$

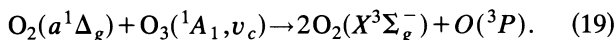
The factor $\phi(T_v)$ reflects the fact that the population of the upper vibrational levels decreases as a result of dissociation processes.

As we have already mentioned, analysis of the experimental data of Ref. 9 shows that $\text{O}_2(a^1\Delta_g)$ production accompanying mixing of the excited oxygen and nitrogen flows occurs with the participation of vibrationally excited ozone, and the $\text{O}_2(a^1\Delta_g)$ production rate in this case is proportional to the O_2 concentration. This suggests that the process resulting in the appearance of the singlet-oxygen molecules is a first-order reaction with respect to the oxygen concentration, and ozone molecules which are vibrationally excited in the asymmetric mode participate in this reaction:



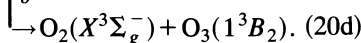
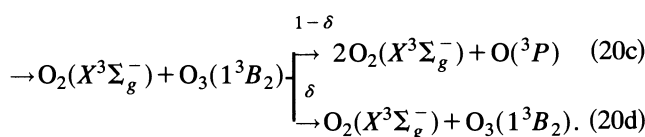
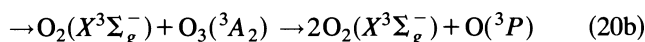
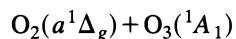
The qualitative agreement between the experimentally measured dynamics of $\text{O}_2(a^1\Delta_g)$ production and the computed vibrational temperature $T_a(t)$ of the asymmetric mode of ozone (see Figs. 2–5a and c) indicates that this vibrational mode of ozone makes the main contribution to the reaction (14). The source of such ozone molecules is three-particle reactions (7) and the vv' exchange processes (1).

The probability of the process (14) ($\Delta v \approx 7$) is low because of the multiple-quantum nature of the process and the total projection of the electron spin is not conserved. However, if the reaction (14) does not proceed directly and the



It is well known that the rate constant of the process (19) is high and increases strongly as ozone is vibrationally excited.²⁹ This suggests that quenching of $\text{O}_2(a^1\Delta_g)$ on O_3 molecules proceeds via the formation of an excited intermediate complex, which decomposes into a $\text{O}_2(X^3\Sigma_g^-)$ molecule and an electronically excited state of ozone, which pre-dissociates into $\text{O}(^3P)$ and $\text{O}_2(X^3\Sigma_g^-)$.

Only the 1^3B_2 excited bound state of ozone is correlated with the system $\text{O}_2(X^3\Sigma_g^-) + \text{O}(^3P)$ (see Fig. 1). The bound state 3B_1 is also correlated with the system $\text{O}_2(a^1\Delta_g) + \text{O}(^3P)$; at energies between the $\text{O}(^3P) + \text{O}_2(X^3\Sigma_g^-)$ and $\text{O}(^3P) + \text{O}_2(a^1\Delta_g)$ dissociation limits the 3B_1 state crosses the 1^3B_2 , 3A_2 , and 1A_2 states (of these, the latter two are unbound). In connection with this arrangement of the electronic states, it can be assumed that the $\text{O}_2(a^1\Delta_g)$ quenching process can proceed via the following channels (20a–20d):

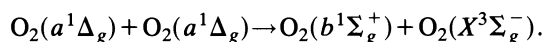


The ratio δ between the channels (20c) and (20d) is determined by the geometry of the O_3 molecules in the input channel of the reaction, i.e., it depends on the vibrational quantum numbers of the ground 1A_1 and excited 1^3B_2 states. According to our estimates $\delta \approx 0.1$, in agreement with the experimental data of Ref. 30.

In the present kinetic model, the rate constants of the inverse reactions, for which the experimentally measured values are unknown, were determined from the principle of detailed balance. Quenching of the excited particles on the walls of the pyrex tube was treated in the diffusion-time approximation.

The complete system of plasma-chemical and vibrational kinetics equations, together with the equation for the gas temperature, was solved using an algorithm for integrating “stiff” systems of ordinary differential equations.

The initial conditions required for solving the system of equations were determined as follows. In the experiment of Ref. 11 the $\text{O}_2(a^1\Delta_g)$ and $\text{O}_2(b^1\Sigma_g^+)$ concentrations and the gas temperature in the mixing zone were measured. Analysis of the experimental results and reactions with the participation of these molecules, immediately in front of the mixing zone of the N_2^* and O_2^* flows, show that the deactivation of $\text{O}_2(a^1\Delta_g)$ and $\text{O}_2(b^1\Sigma_g^+)$ was completely determined by collisions with ozone molecules, and $\text{O}_2(b^1\Sigma_g^+)$ production occurred via the binary reaction



This made it possible to obtain quite accurate estimates of the O_3 concentrations in the mixing zone.

The initial conditions for components which were not recorded in the experiment were determined by modeling hf discharges and the postdischarge stage during the transport of ozone and oxygen fluxes to the mixing zone.

A number of parameters, describing the flow of reactions in which electronically and vibrationally excited ozone molecules participate, were introduced into the model. Because the reaction rate constants are exponential functions of the vibrational temperatures, the dynamics of the main components of the mixture was strongly affected by a change in the values of these parameters. This made it possible, by comparing the experimental data with the computational results, to determine a single set of model parameters.

3. COMPUTATIONAL RESULTS AND DISCUSSION

Figures 2–5 display the typical computational dependences: a) $\text{O}_2(a^1\Delta_g)$ concentration, b) $\text{O}(^3P)$ and O_3 concentrations, and c) the vibrational temperatures T_a , T_s , and T_n as functions of time after the nitrogen and oxygen flows are mixed in the ratios $\text{N}_2:\text{O}_2 = 4:1, 9:1, 19:1, \text{ and } 39:1$, respectively. The total pressure was 10 torr. The specific energy input in the hf discharge plasma reached $\approx 1 \text{ J/cm}^3 \cdot \text{atm}$.

Figures 2a–5a display the experimental curves¹¹ of the dynamics $[\text{O}_2(a^1\Delta_g)](t)$ in a mixture of flows of excited oxygen and excited nitrogen (filled circles) as well as flows of excited oxygen and unexcited nitrogen (open circles). One can see that for the same mixtures these dependences differ appreciably, and the addition of excited nitrogen increases the $\text{O}_2(a^1\Delta_g)$ concentration in the mixture by 10–50%. In the experimental determination of the $\text{O}_2(a^1\Delta_g)$ concentration,¹¹ the error is at most 1–2%, which is consistent with the spread in the experimental points in Figs. 2a–5a.

The relationship between the dynamics of the singlet-oxygen concentration and the vibrational temperatures T_a and T_s of the ozone molecules after the excited N_2 and O_2 flows are mixed can be determined by analyzing simultaneously $\text{O}_2(a^1\Delta_g)$ and O_3 production and destruction processes.

3.1. Dynamics of the excitation of the vibrational modes of ozone molecules

As we have already mentioned, over the time it takes the oxygen excited in an hf discharge to reach the mixing zone (t_{tr}), all of the atomic oxygen is converted into ozone, which is produced in a vibrationally excited state. The relaxation time of this excitation is much shorter than t_{tr} , and for this reason, immediately prior to mixing of the oxygen and nitrogen flows, the ozone vibrational temperatures T_a and T_s are equal to the gas temperature.

We shall now analyze the computational results, displayed in Figs. 2c–5c, for the dynamics of the excitation of the O_3 vibrational modes. After the N_2^* in O_2^* fluxes mix, vibrations in the asymmetric mode of ozone are excited in $\nu\nu'$ exchange processes between nitrogen and ozone [the reactions (1)]. This excitation stimulates O_3 dissociation in the processes (8) accompanied by the production of atomic oxygen $\text{O}(^3P)$. For $[\text{O}(^3P)]/[\text{M}] > 0.3\%$, where

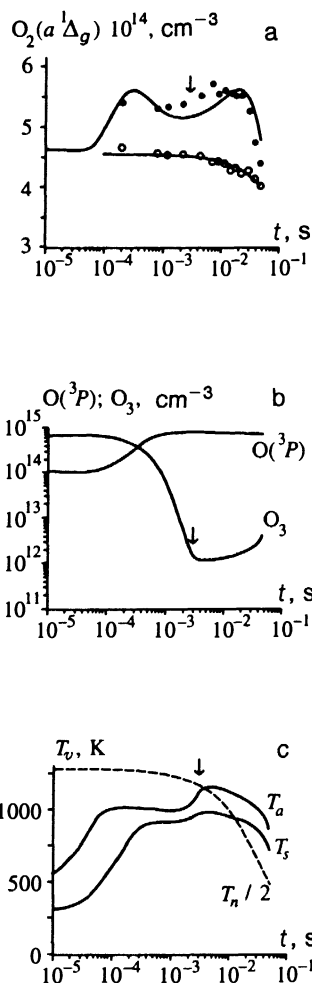
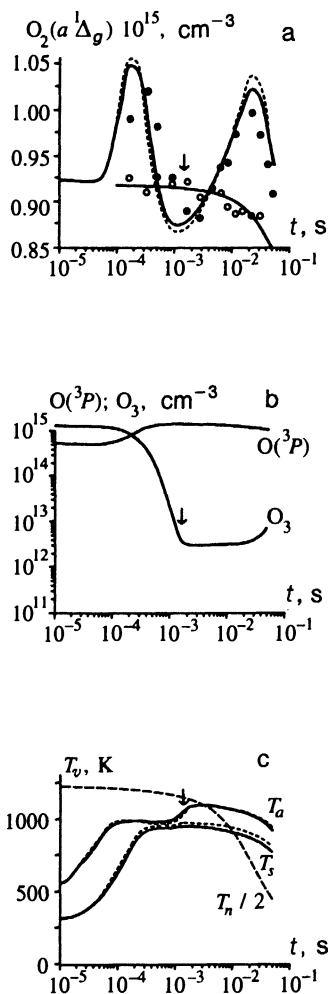


FIG. 2. (a) $O_2(a^1\Delta_g)$ concentration, (b) $O(^3P)$ and O_3 , and (c) vibrational temperatures of the asymmetric (T_a) and symmetric (T_s) modes of O_3 as a function of time after mixing of the nitrogen and oxygen flows in the ratio $N_2 : O_2 = 4:1$; $P = 10$ torr. The open and filled circles represent the experimental data^{9,10} obtained by mixing fluxes of excited oxygen with excited and unexcited nitrogen, respectively. The solid lines represent the computational results obtained in the harmonic-oscillator approximation; the short-dash lines represent the computational results obtained taking into account anharmonicity; and the long-dash line represents the time dependence of the vibrational temperature of nitrogen ($T_n/2$).

FIG. 3. Same for the mixture $N_2 : O_2 = 9:1$. The long-dash lines represent the time dependence of the vibrational temperature of nitrogen ($T_n/2$).

$M = N_2, O_2$, an increase of the $O(^3P)$ concentration results in an increase of the characteristic frequency of O_3 intermode exchange. This condition holds only for the mixtures $N_2 : O_2 = 4:1$ and $9:1$. For this reason, at times $t = 0.3 - 1$ ms, the quasistationary values of T_a are lower and those of T_s are higher for these mixtures than for mixtures with a lower oxygen fraction. The quantities T_a and T_s remain constant as long as $O_3(v_a)$ vibrations are excited mainly via vv' exchange with nitrogen molecules. As the ozone concentration decreases, the contribution of this excitation channel decreases and, as a result, the contribution of three-particle ozone production reactions increases. The rates of the processes (7) and (1) become equal when $[O_3] = [O_3]^*$, where

$$[O_3]^* = sK_7[O][O_2][M]/(K_1[N_2(\nu=1)]),$$

$$M = N_2, O_2,$$

here s is the ratio of the numbers of the vibrational quanta of the asymmetric mode of O_3 , which are produced in the reactions (7) and (1), respectively. Therefore, for $[O_3] < [O_3]^*$ the condition $Q_{vv}^{na} < F^a$ is satisfied for the terms on the right-hand side of Eq. (5).

The decrease of the vibrational quanta stored in the asymmetric mode of O_3 is determined by $O_3(v_a)$ intermode exchange and dissociation processes (8), dissociation being the predominant channel for $T_a > T_a^* \approx 1000$ K. One can see from Figs. 2c–5c that the latter condition holds at times $t > (5-6) \cdot 10^{-4}$ s, so that in Eq. (5) $D^a > Q_{vv}^{as} + P_{vT}^a$.

Under the conditions considered, when $[O_3] < [O_3]^*$, the degree of vibrational excitation of ozone and the quantity T_a are found to depend on the ratio $\eta = [O(^3P)]/[O_3]$. As the values of T_a increase, the vibrational temperature of O_3 reaches the critical value T_a^* , at which the dissociation of ozone molecules in the asymmetric vibrational mode in the reactions (8) proceeds just as quickly as intermode exchange with the symmetric mode of O_3 . Ultimately, when $T_a > T_a^*$ holds, a situation arises when an increase of the ratio η results in an increase of T_a , and this, in turn, results in acceleration of O_3 dissociation and further growth of η . Since these processes are interrelated, positive feedback occurs. We

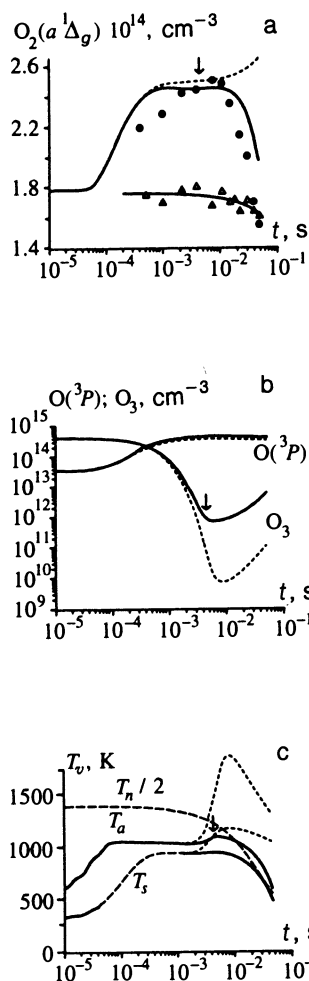


FIG. 4. Same for the mixture $N_2:O_2 = 19:1$. The short-dash lines represent the computational results for $\phi(T_v) = 1$. See text for an explanation of the notation.

term this a “vibrational explosion.” The time corresponding to the “explosion” is marked in the figures by an arrow.

If it is assumed that for terms on the right-hand side of Eq. (5) the conditions $D^a \gg Q_{vv}^{as} + P_{vT}$ and $F^a \gg Q_{vv}^{na}$ are satisfied, then linearizing the equation obtained and the equation for the rate of change of the ozone concentration, we obtain an estimate for the growth rate of the “vibrational explosion” ($T_a \sim \exp(\gamma t)$):

$$\gamma \approx \nu_0 \frac{E_{act}^{eff}}{kT_a^*} \exp\left\{-\frac{E_{act}^{eff}}{kT_a^*}\right\},$$

ν_0 is the frequency of gas-kinetic collisions, E_{act}^{eff} is the effective activation barrier in ozone decomposition reactions (8), and T_a^* is the critical vibrational temperature of the asymmetric mode.

As the vibrational temperature T_a increases, processes leading to the dissociation of $O_3(v_a)$ molecules start to influence strongly the form of the vibrational distribution function of O_3 in high vibrational levels. This influence was taken into account by introducing corresponding corrections into the expression for the dependence of the rate constants of processes with high energy barriers on the vibrational ex-

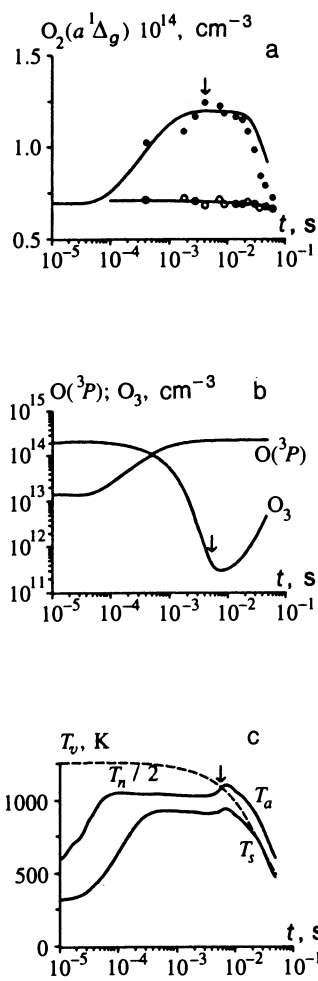


FIG. 5. Same for the mixture $N_2:O_2 = 39:1$.

citation of the reagents. In particular, the expressions (12)–(13) were used for O_3 collisional dissociation processes (8).

The presence of the factor $\phi(T_v)$ in Eq. (12) is associated with the appearance of a dependence of the ozone dissociation rate constant on the ratio of the rates of vv exchange and dissociation of O_3 . When this ratio decreases, the populations of the upper vibrational levels of O_3 decrease as a result of dissociation, and this results in lower values of K_D .

Therefore, as T_a and the concentration of ozone molecules decrease (Figs. 2–5), the values of $\phi(T_a)$ and K_D (T_a) decrease appreciably. Ultimately, this results in a decrease of the O_3 decomposition rate and a change in the sign of the derivative $d[O_3]/dt$.

The computational results displayed in Figs. 2–5 were obtained for values of $\phi(T_v)$ determined by the expression (13). Figure 4 displays calculations for the case $\phi(T_v) = 1$ (dashed lines). As one can see, if we drop the effect of dissociation processes on the form of the vibrational distribution function of O_3 by setting $\phi(T_{a,s}) = 1$, then the explosive growth of the vibrational temperatures T_a and T_s saturates at much higher values of these temperatures. Moreover, the maximum degree of dissociation of the ozone molecules increases by a factor of 10 and the dynamics of

$[O_2(a^1\Delta_g)](t)$ is qualitatively different after the “vibrational explosion.”

The growth of the vibrational temperature T_a saturates for the following reason. It follows from Eq. (5) for the number of vibrational quanta stored in the asymmetric mode of O_3 that the intensity of pumping of vibrations in the reactions (7) does not change much over the time of the “explosion.” At the same time, the quantity D^a , determined by the rate of the process of dissociation of $O_3(v_a)$ molecules, increases significantly with increasing T_a as a result of the exponential growth of the constants of the reactions (8). Ultimately, when a stationary value T_a^{st} is reached, the derivative da/dt becomes equal to zero. Then, the ozone concentration is such that the O_3 production and decomposition processes are balanced.

As we have already mentioned above, ozone dissociates mainly via the processes (8), stimulated by vibrational excitation of the asymmetric mode of O_3 . However, for mixtures with a high oxygen content and, correspondingly, high $O_2(a^1\Delta_g)$ concentration (for example, $N_2 : O_2 = 4:1$, Fig. 2), the reaction leading to decomposition of O_3 on $O_2(a^1\Delta_g)$ (22) is also important. In this case, the characteristic O_3 dissociation times are almost two times shorter than the corresponding times for mixtures with a low oxygen content. Ultimately, the times at which the condition $[O_3] < [O_3]^*$ holds and T_a starts to increase are shorter for the mixture $N_2 : O_2 = 4:1$ (Fig. 2) than for the mixtures 19:1 (Fig. 4) and 39:1 (Fig. 5). In the latter two cases, these times are comparable in magnitude to the relaxation time of N_2 vibrational excitation at the walls of the discharge tube.

The effect of relaxation of N_2 vibrations on $T_a(t)$ dynamics is different for different mixtures and depends on the magnitude of the channel corresponding to the contribution of the vv' exchange with nitrogen to the vibrational excitation of $O_3(v_a)$. For mixtures with a low oxygen content, when the contributions of this channel and the three-particle O_3 production reactions are comparable in magnitude, a decrease of T_n results in a decrease of T_a and T_s (Figs. 4c, 5c). At the same time, for the mixtures $N_2 : O_2 = 4:1$ and 9:1, a decrease of T_n has a weaker effect on the $T_a(t)$ dynamics. The main channel for $O_3(v_a)$ relaxation at this stage is intermode exchange in O_3 ; this results in the excitation of the deformational mode of ozone. The usual time for the deformation mode is $\sim 0.1 \mu s$. As a result of this, the vibrational temperature T_s reaches its quasistationary value after T_a becomes stationary (Figs. 2c–5c).

3.2. Dynamics of the production of singlet-oxygen molecules

After the flows of excited oxygen and unexcited nitrogen mix (open circles in Figs. 2a–5a), the $O_2(a^1\Delta_g)$ concentration changes very little at times $t \leq 10^{-2}$ s. This is associated with the fact that the deactivation of this state on unexcited ozone molecules is slow.

The mixing of the excited oxygen and nitrogen fluxes, as has already been mentioned, results in filling of the asymmetric vibrations of O_3 and growth of T_a and T_s (Figs. 2c–5c). An increase of the vibrational temperature T_a stimulates

$O_2(a^1\Delta_g)$ production in reactions of $O_3(1^3B_2)$ with oxygen (15). As a result, for $t \leq 50 \mu s$ the $O_2(a^1\Delta_g)$ concentration increases. The temporal resolution of the experiment of Ref. 9 (~ 0.2 ms) made it impossible to record fast $O_2(a^1\Delta_g)$ production and destruction processes immediately after mixing. Modeling showed, however, that in all of the mixtures considered, at times $t < 0.3$ ms, the vibrational temperatures T_a and T_s and the $O_2(a^1\Delta_g)$ concentration behave similarly as functions of the time.

The dynamics of the $O_2(a^1\Delta_g)$ concentration is described by the equation

$$\frac{d[O_2(a^1\Delta_g)]}{dt} = [O_3(v_a)][O_2]K_8 - [O_2(a^1\Delta_g)]([O_3(v_c)]K_{22} + O(^3P)]K_{23}, \quad (21)$$

where

$$O_2(a^1\Delta_g) + O_3(vib) \rightarrow O(^3P) + 2O_2(X^3\Sigma_g^-), \quad (22)$$

$$K_{22} = 5.2 \cdot 10^{-11} \exp\left(-\frac{2840}{T_s}\right),$$

$$O_2(a^1\Sigma_g) + O(^3P) \rightarrow O(^3P) + O_2(X^3\Sigma_g^-), \quad (23)$$

$$K_{23} = 1.3 \cdot 10^{-16} \text{ cm}^3/\text{s}.$$

Comparing the quench rates K_{22} and K_{23} shows that $O_2(a^1\Delta_g)$ deactivation is determined by the reaction (22) and depends strongly on the vibrational temperature T_s of the symmetric mode of ozone.

The main $O_2(a^1\Delta_g)$ production channel is quenching of $O_3(1^3B_2)$ by oxygen (15). The concentrations of $O_3(1^3B_2)$ and vibrationally excited ozone molecules in the ground state $O_3(1^1A_1, v_a)$ are related by the relation (17). For this reason, the character of the function $[O_2(a^1\Delta_g)](t)$ depends on the ratio of the vibrational temperatures T_a and T_s , whose values determine the rates of the reactions (15) and (22), respectively. The characteristic values of the $O_3(1^3B_2)$ concentrations for $t \geq 10^{-4}$ s are $10^{11} - 10^{12} \text{ cm}^{-3}$.

The vibrational temperature T_a reaches a quasistationary value at times $t \geq (5-7) \cdot 10^{-4}$ s, while T_s continues to grow. As a result of this, the derivative $d[O_2(a^1\Delta_g)]/dt$ at first decreases to zero and then becomes negative. The absolute values of the derivative increase as the oxygen fraction in the mixture increases.

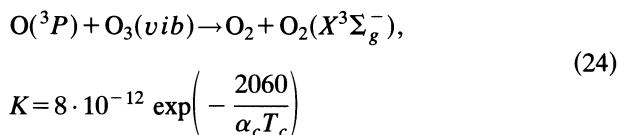
The “explosive” growth of the vibrational temperature T_a , described in the preceding section, results in acceleration of the $O_2(a^1\Delta_g)$ production reactions (15). The concentration of singlet oxygen increases. The “vibrational explosion” is immediately followed by a decrease of the vibrational temperature T_a (Figs. 2c–5c). As a result, the sign of the derivative $d[O_2(a^1\Delta_g)]/dt$ changes once again and a second maximum appears in the curve $[O_2(a^1\Delta_g)](t)$ (Figs. 2a–3a). The amplitude of this maximum decreases appreciably as the oxygen fraction in the mixture decreases, but the character of the time dependence of the $O_2(a^1\Delta_g)$ concentration does not change, since the character of the relative change of T_a and T_s remains the same.

As follows from Eq. (21), the derivative $d[\text{O}_2(a^1\Delta_g)]/dt$ is proportional to the concentration $[\text{O}_3(t)]$, which depends on the initial value $[\text{O}_3(t=0)]$. As we have already noted above, the initial values of the ozone concentration in front of the mixing zone were determined on the basis of experimental data on the $\text{O}_2(a^1\Delta_g)$ and $\text{O}_2(b^1\Sigma_g^+)$ deactivation rates.^{11,12} These values agree well with the computational results for all mixtures investigated.

We obtained our main results by using the harmonic-oscillator approximation for the vibrational modes of ozone. Taking into account anharmonicity in the equations of vibrational and chemical kinetics did not change the qualitative picture of the dynamics of $[\text{O}_2(a^1\Delta_g)]$ and of the O_3 vibrational temperatures. The computational results, illustrating the effective anharmonicity of the vibrations of ozone molecules, are presented in Figs. 2a and 2c (dashed lines).

The values of the model parameters were obtained by matching the results of a series of calculations to the experimental data. This enabled us to use a single set of parameters to describe all experimental results.

Under the conditions considered, the influence of the process



on the $\text{O}_2(a^1\Delta_g)$ kinetics and the ozone vibrational kinetics was insignificant. This made it difficult to determine the role of any particular mode of ozone in the acceleration of these processes. The best quantitative agreement between the computational and experimental results was obtained by assuming that the reactions (24) are accelerated by the excitation of the symmetric O_3 vibrational mode with the vibrational excitation utilization factor $\alpha_c \approx 0.3 \pm 0.2$. The value obtained for the coefficient α_c agrees with the data of Ref. 31.

The value obtained for the rate constant of $\nu\nu'$ exchange between $\text{N}_2(\nu=1)$ and $\text{O}_3(101)$ [reaction (1)] was found to be $K_1 = (5 \pm 2) \cdot 10^{-14} \text{ cm}^3/\text{s}$. It agrees with the value, presented in Ref. 6, for the effective rate constant of energy transfer from vibrational degrees of freedom of nitrogen into the electronic state $a^1\Delta_g$ of the oxygen molecule. The best agreement between the theoretical and experimental results was obtained for $\delta\varepsilon \approx 0.45 \pm 0.05 \text{ eV}$, which is somewhat smaller than the value $\delta\varepsilon \sim 0.05\text{--}0.6 \text{ eV}$ obtained in Refs. 22 and 23. The effective vibrational level ν_a of the asymmetric mode of O_3 , above which the ozone electronic states 1A_1 and 3B_2 are assumed to be strongly coupled, was found to be close to the $\text{O}_2(X^3\Sigma_g^-) + \text{O}(^3P)$ dissociation threshold (in the harmonic approximation $\nu_a \approx 7$). The rate constant for quasiresonant transfer of electronic excitation from $\text{O}_3(^3B_2)$ to $\text{O}_2(a^1\Delta_g)$ (15), determined to within the factor $P^+/P^- \approx 1$, was found to be $(1.4 \pm 0.5) \cdot 10^{-12} \text{ cm}^3/\text{s}$. This value agrees with the data of Refs. 14 and 15 for the rate of this process in the $\text{NO}_2(^2B_2)\text{--}\text{O}_2(a^1\Delta_g)$ system.

Note that the description of the ozone dissociation process on the basis of the given form of the O_3 vibrational distribution function is not entirely correct. At the present time, however, full-scale numerical modeling of the kinetics

of individual levels in the system of O_3 vibrational modes is complicated by the lack of data on the rates of $\nu\nu$ and $\nu\nu'$ exchange on high vibrational levels of different modes of O_3 .

4. CONCLUSIONS

In the present paper we have presented a theoretical model of the production of singlet-oxygen $\text{O}_2(a^1\Delta_g)$ molecules in strongly excited nitrogen–oxygen gas media. The model was developed on the basis of results obtained in a series of experimental and theoretical investigations which we performed.^{7–12}

The model is based on a new mechanism of excitation of the lower singlet level of oxygen by transfer of energy during the interaction of electronically excited state 1^3B_2 of ozone with oxygen molecules. The ozone molecules appearing in high vibrational levels in the asymmetric mode ($\nu_a \geq 7$) are transformed into this electronic state by nonadiabatic transitions.

It was found that vibrationally excited nitrogen plays an important role as a reservoir for asymmetric vibrations of ozone. It was also shown that acceleration of $\text{O}_2(a^1\Delta_g)$ quenching in reactions with ozone is associated with the excitation of the O_3 bending vibrations (symmetric mode). This reaction probably proceeds via the excitation of the intermediate electronic state $\text{O}_3(^3B_2)$. The rate constants of the processes studied were determined by comparing the results of modeling to existing experimental data.

As mentioned above, the model is based on a large quantity of experimental data on the kinetics of $\text{O}_2(a^1\Delta_g)$. The lack of experimental data on $\text{O}_3(^3B_2)$ diagnostics under the same conditions raises the question of performing additional investigations to check the basic assumptions of the theory developed.

Financial support for this work was provided by the Russian Fund for Fundamental Research.

¹R. P. Wayne, *J. Photochem.* **25**, 345 (1984).

²W. E. McDermott, N. R. Pchelkin, D. J. Bernard, and R. R. Bousek, *Appl. Phys. Lett.* **32**, 469 (1978).

³K. Tachibana and A. V. Phelps, *J. Chem. Phys.* **75**, 3315 (1981).

⁴C. Yamabe and A. V. Phelps, *J. Chem. Phys.* **78**, 2984 (1983).

⁵S. A. Lawton and A. V. Phelps, *J. Chem. Phys.* **69**, 1055 (1978).

⁶A. N. Vasil'eva, I. A. Grishina, K. S. Klopovskii *et al.*, *Fiz. Plazmy* **15**, 190 (1989) [*Sov. J. Plasma Phys.* **15**, 108 (1989)].

⁷A. B. Abishev, M. L. Belov, K. S. Klopovskii *et al.*, *Fiz. Plazmy* **16**, 844 (1990) [*Sov. J. Plasma Phys.* **16**, 490 (1990)].

⁸A. M. Popov, A. T. Rakhimov, and T. V. Rakhimova, *Fiz. Plazmy* **19**, 1241 (1993) [*Sov. J. Plasma Phys.* **19**, 651 (1993)].

⁹V. A. Feoktistov, D. V. Lopaev, K. S. Klopovsky *et al.*, *J. Nucl. Mater.* **200**, 309 (1993).

¹⁰A. A. Blyablin, A. N. Vasil'eva, A. S. Kovalev, and D. V. Lopaev, *Fiz. Plazmy* **15**, 1012 (1989) [*Sov. J. Plasma Phys.* **15**, 587 (1989)].

¹¹K. S. Klopovskii, A. S. Kovalev, D. V. Lopaev *et al.*, *Fiz. Plazmy* **18**, 1606 (1992) [*Sov. J. Plasma Phys.* **18**, 834 (1992)].

¹²D. V. Lopaev, Candidate's Dissertation in Physical-Mathematical Sciences, Scientific-Research Institute of Nuclear Physics, Moscow State University, Moscow, 1993.

¹³A. A. Ali, E. A. Ogryzlo, Y. Q. Shen, and P. T. Wassell, *Can. J. Phys.* **64**, 1614 (1986).

¹⁴I. T. N. Jones and K. D. Bayes, *J. Chem. Phys.* **59**, 3119 (1973).

¹⁵T. C. Frankiewicz and R. S. Berry, *J. Chem. Phys.* **58**, 1787 (1973).

¹⁶A. Barbe, C. Secroun, and P. Jouve, *J. Mol. Spectrosc.* **49**, 171 (1974).

- ¹⁷A. A. Radtsig and B. M. Smirnov, *Reference Data on Atoms, Molecules, and Ions*, Springer-Verlag, N. Y., 1985.
- ¹⁸F. Menard-Bourcin, J. Menard, and L. Doyennette, *J. Chem. Phys.* **94**, 1875 (1991).
- ¹⁹J. I. Steinfeld, S. M. Adler-Golden, and J. W. Gallagher, *J. Phys. Chem. Ref. Data* **16**, 911 (1987).
- ²⁰V. D. Rusanov and A. A. Fridman, *The Physics of a Chemically Active Plasma* [in Russian], Nauka, Moscow, 1984.
- ²¹T. Kleindienst, J. B. Burkholder, and E. J. Bair, *Chem. Phys. Lett.* **70**, 117 (1980).
- ²²W. T. Rawlins and R. A. Armstrong, *J. Chem. Phys.* **87**, 5202 (1987).
- ²³W. T. Rawlins, G. E. Caledonia, and R. A. Armstrong, *J. Chem. Phys.* **87**, 5209 (1987).
- ²⁴S. S. Xantheas, G. J. Atchity, S. T. Elbert, and K. Ruedenberg, *J. Chem. Phys.* **94**, 8054 (1991).
- ²⁵A. Banichevich and S. D. Peyerimoff, *Chem. Phys.* **174**, 93 (1993).
- ²⁶P. J. Hay and T. H. Dunning, *J. Chem. Phys.* **67**, 2290 (1977).
- ²⁷R. O. Jones, *J. Chem. Phys.* **82**, 325 (1985).
- ²⁸C. W. Wilson and D. G. Hopper Jr., *J. Chem. Phys.* **74**, 595 (1981).
- ²⁹M. J. Kurylo, W. Braun, A. Kaldor *et al.*, *J. Photochem.* **3**, 71 (1974).
- ³⁰F. D. Findlay and D. R. Shelling, *J. Chem. Phys.* **54**, 2750 (1971).
- ³¹S. D. Il'in, V. V. Selikhanovich, Yu. M. Gershenzon, and V. B. Rozen-shtein, *Khim. Fiz.* **10**, 1060 (1991).

Translated by M. E. Alferieff